Materials Research Proceedings 29 (2023) 416-424 https://doi.org/10.21741/9781644902516-47

Dry reforming of methane over Ni/KCC-1 catalyst for syngas production

SITI NUR SABIHA Suhaimi[1,a], SYED MUHAMMAD WAJAHAT Ul Hasnain [1,b], AHMAD Salam Farooqi[1,2,c], HERMA Dina Setiabudi[3,d], SYED Anuar Faua'ad Syed Muhammad[4,e], SHAHRUL Ismail[5,f], BAWADI Abdullah[1,2,g*]

[1]Department of Chemical Engineering, Universiti Teknologi PETRONAS, Seri Iskandar, 32610, Perak, Malaysia

[2]Centre of Contamination Control and Utilization (CenCoU), Universiti Teknologi PETRONAS, Seri Iskandar, 32610, Perak, Malaysia

[3]Faculty of Chemical and Process Engineering Technology, College of Engineering Technology, Universiti Malaysia Pahang, 26300 Gambang, Kuantan, Pahang, Malaysia

[4]School of Chemical and Energy Engineering, Faculty of Engineering, Universiti Teknologi Malaysia, UTM Skudai, 81310 Skudai, Johor, Malaysia

[5]School of Ocean Engineering, Universiti Malaysia Terengganu, 21030 Kuala Nerus, Terengganu, Malaysia

[a]siti.nur_24455@utp.edu.my, [b]syed_22000103@utp.edu.my, [c]ahmad.farooqi@utp.edu.my, [d]herma@ump.edu.my, [e]syed@utm.my, [f]shahrul.ismail@umt.edu.my, [g]bawadi_abdullah@utp.edu.my

Keywords: Catalyst Development, Ni-Based Catalysts, Syngas Production, KCC-1

Abstract. Dry reforming of methane (DRM) is a trendy topic of investigation as a means of reducing global warming. However, the adoption of DRM for a commercial purpose is still a question due to the deactivation and sintering of catalysts. The performance of the 5Ni/KCC-1 catalyst by using the ultrasonic-assisted impregnation method was examined in this study. The micro-emulsion method and ultrasonic-assisted impregnation method were used to prepare KCC-1 support and 5Ni/KCC-1 catalyst respectively. The catalyst was characterized by N_2 adsorption-desorption and field emission scanning electron microscopy (FESEM) techniques. FESEM morphology shows that KCC-1 support experienced a well-defined fibrous morphology in a uniform microsphere which can promote high catalytic activity. The results show that the catalyst has optimum performance with higher reactant conversions and H_2/CO ratio when operated at 850ºC in a tubular furnace reactor as compared to 750ºC.

Introduction

The recent global temperature rise is closely related to increased anthropogenic greenhouse gas emissions over the past century. The most common greenhouse gases are methane (CH_4) and carbon dioxide (CO_2) and they are the major developer of the recent problems of climate change [1]. This has resulted in greenhouse gas (GHG) accumulation such as CH_4 and CO_2 that induces a global climate change that triggers extreme natural phenomena effects such as heavy floods in some areas and severe droughts in other parts of the world that have intensified environmental pressure, thereby impacting biodiversity [2], [3].

Emissions of methane from natural causes such as termites, grasslands, wildfires, wetlands and lakes while human activities such as the refining of oil and gas from coal mines and agricultural activities [4]. This has resulted in greenhouse gas (GHG) accumulation such as CH_4 and CO_2 that

induces a global climate change that triggers extreme natural phenomena effects such as heavy floods in some areas and severe droughts in other parts of the world that have intensified environmental pressure, thereby impacting biodiversity [5], [6].

Fossil fuels are the most important source of CO_2 emissions, with the most significant contribution to this energy paradigm [7]. In addition, human activities in industries such as textiles, aluminum, pulp and paper, refineries, cement, iron and steel, and landfills also result in excess atmospheric CO_2 pollution due to the conversion of raw materials. According to the United States Environmental Protection Agency, there is inadequate natural removal of CO_2 from forests and oceans to remove excess CO_2 from the atmosphere [8]. Renewable energy may serve as alternatives to fossil fuels that alleviate this challenge, such as hydropower, wind and solar power, but these sources depend on geographical, nocturnal and seasonal variations. In green energy science, reducing greenhouse gas emissions has become one of the most important challenges in minimizing temperature increases and coping with global warming [9], [10]. The conversion of two greenhouse gases, methane and carbon dioxide, into a value-added product called synthetic gas, can be accomplished by methane steam reforming (SRM), methane partial oxidation (POM) and methane dry reforming (DRM). Synthetic gas is a combination of two gases containing hydrogen (H_2) and carbon monoxide (CO), known as syngas [11], [12].

DRM is used due to its, lower cost, environmentally friendly, and effective energy utilization. In the DRM process, the catalyst is the main existence as it is responsible for changing the reaction rate, and improving syngas production without being consumed in it [13]. However, coke deposition and catalyst sintering at high temperatures are the main challenges in this reaction [14]. These two problems can cause the catalyst to be deactivated. Therefore the discovery of the extremely active and stable catalyst used in DRM is of great importance [15]. The addition of mesoporous silica particle (KCC-1) into Ni-based catalyst is being studied in this project. The high accessibility to the active sites of the bulky mass reactant is one of the advantages of this fibrous morphology, thus increasing the reaction rate and the formation of the material [16]. Oxygen vacancy has recently been regarded as one of the reactive sites in the methanation process and the rate of action is significantly improved by adsorbing and activating the carbon-oxygen bond [17].

Thus, the primary aim of this research is to study the influence of KCC-1 support over Ni catalyst on the catalytic performance during the DRM reaction. The freshly prepared catalyst was studied by BET technique. The DRM reaction was conducted at 700 ℃ and 800 ℃ under atmospheric pressure by feeding CH_4, CO_2 at a stoichiometric ratio of 1:1 respectively.

Materials and methods

Catalyst Synthesis. The catalyst support KCC-1 was synthesized by a micro-emulsion method. For this, tetraethyl orthosilicate, butanol, and toluene are stirred in a beaker for 30 minutes at a temperature 30 °C while urea, cetyl tri ammonium bromide (CTAB, Aldrich), and water were stirred in another beaker for 30 minutes at temperature 30 °C. Both solutions were then mixed, and stirred for 45 minutes at 30 °C. After that, the solution was heated in a Teflon-sealed hydrothermal reactor for 5 hours at 120 °C. The obtained solution is centrifuged, rinsed, and oven-dried for 12 h at a temperature 100 °C and calcined for 5 hours at 550 °C.

In the next step, the Ni was impregnated onto the support KCC-1 by the ultrasonic-assisted impregnation method. The necessary amount of $Ni(NO_3)_2 \cdot 6H_2O$ was dissolved in diluted water to make the aqueous solution and then mixed with the calculated amount of the support. The resulting slurry was then immersed in the ultrasonic cleaner bath and heated slowly at 80°C until nearly all the water had evaporated. The solid residue was dried overnight at 110°C followed by calcination at 550°C for 3 h.

Catalyst Characterization. At 77 K, a gas adsorption analyzer (Tristar 3020, Micromeritics) was used to measure the textural properties of catalysts using an N_2 physisorption isotherm. The BET

Materials Research Proceedings 29 (2023) 416-424 https://doi.org/10.21741/9781644902516-47

method by relative pressure range (p/po) of 0.05 – 0.20 was used to calculate particular surface areas. While the amount of N2 absorbed in a relative pressure range (p/po) was used to calculate pore volumes. The morphologies of the catalyst were observed by using the FESEM technique. XRD was used to determine the composition and structure of the catalyst. Powder X-ray diffraction patterns with a Bruker D8B Advance X-ray diffractometer are reported on the calcined catalysts in which Cu-Kα at a wavelength of 1.54Å was used. With an exposure time of 3 seconds and a step size of 1°, the XRD had a scanning range of 10-90°.

Catalyst Evaluation. The catalyst was tested in the tubular reactor to perform a DRM reaction. The catalyst was placed in the catalyst tube, which was made from quartz with 10 mm internal diameter. To hold the catalyst in a catalyst tube, 100 mg of catalyst was packed between two glass wool. the catalyst was purged with nitrogen at 30 mL min^{-1} at a temperature 750 °C. After 1 hour of purging, hydrogen gas was added to the catalyst bed with the same flow rate 30 mL min^{-1} at the same temperature of 750°C. This means a flow of H_2 and N_2 into the catalyst bed is 50% each to reduce the catalyst for catalyst activation. A reduction process was carried out for 3 h. After that, the catalyst bed was purged back with 20 mL min^{-1} to remove all hydrogen gas presence during reduction. Reactants were fed into the catalyst bed with an equimolar rate at 60 mL min^{-1} in a ratio of 1:1:1 for CH_4:CO_2:N_2 at a temperature of 750°C and atmospheric pressure. The catalyst activity was observed for 6 hours on stream. Online gas chromatography was used to continuously monitor and analyzed the excess reactant and product gases of hydrogen and carbon monoxide. The same procedure was repeated for the temperature at 850°C. The conversions of the gases were calculated by using the following equation:

$$CH_4\ (\%) = \left(\frac{F_{CH4,in} - F_{CH4,out}}{F_{CH4,in}}\right) \times 100 \quad (1)$$

$$CO_2\ (\%) = \left(\frac{F_{CO2,in} - F_{CO2,out}}{F_{CO2,in}}\right) \times 100 \quad (2)$$

$$\frac{H_2}{CO} = \frac{F_{H2,out}}{F_{CO,out}} \quad (3)$$

Where F_{in} and F_{out} are the molar flowrates ($mol.s^{-1}$) of the gases going in and out of the reactor.

Results and Discussion

N_2 Physisorption Analysis. The table below shows the N_2 adsorption-desorption isotherms and pore size distributions of 5Ni/KCC-1 catalysts. The 5Ni/KCC-1 catalyst performed type IV isotherm due to the average pore diameter is 8.68 nm, which falls under the range of mesoporous material (2-50 nm). The type IV isotherm occurs at pressures below the gas saturation pressure. It shows the formation of a monolayer followed by the formation of multilayers at lower pressures. The 5Ni/KCC-1 catalyst experienced H3 hysteresis loops as it can be thought of as a middle ground between adsorption and desorption limit forms. The relative pressure (p/po) of 5Ni/KCC-1 is also high which is from 0.8 to 1.0 causing the aggregates of plate-like particles to produce slit-shaped pores resulting the type H3 hysteresis loop. The average pore diameter of the 5Ni/KCC-1 catalyst is 8.68 showing that this catalyst a has high value of pore diameter. The surface area and pore volume of this catalyst are 456.6031 m_2/g and 0.991964 cm^3/g respectively. This can cause an increasing activity of KCC-1 due to its fibrous morphology, big pore size and large surface area.

Table 1 Textural properties of 5Ni/KCC-1 catalyst

Sample	BET Surface Area (m^2/g)	Pore Volume (cm^3/g)	Average Pore Diameter (nm)	Isotherm Type
5Ni/KCC-1	456.6031	0.991964	8.68614	IV

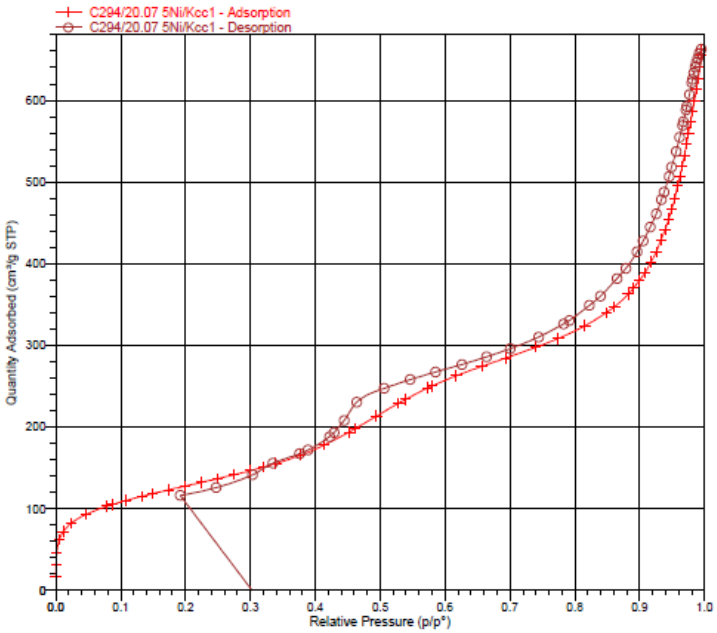

Fig. 1 N_2 adsorption-desorption isotherm curves

FESEM analysis. The morphologies of the Ni/ KCC-1 sample was studied using a Field Emission Scanning Electron Microscope (FESEM). The magnification of sample testing are 10000, 20000, 30000 and 100000. The distribution of Ni metals on the fibrous KCC-1 support can be seen via FESEM micrographs as shown in Figure 2. The dispersion of Ni grains is represented by the white spots and it sticks on the wall of the KCC-1 without uniform shape. The FESEM imaging also shows that Ni metal is well dispersed on the KCC-1 support without the agglomeration. While the formation of the fibrous KCC-1 structures is expected to be a well-defined fibrous morphology in a uniform microsphere in the range of size 202.7-790.1 nm. As shown in Figure 2, mesoporous silica KCC-1 also has a structure of big pores and dendrimers that are radially symmetric molecules with a well-defined, homogenous and monodisperse structure that has a typically symmetric core. This is due to the distance between each specific dendrimer, the reactant was able to diffuse easily, allowing for high catalytic performance [18]. Additionally, the ultrasonic-assisted impregnation technique showed that the fibrous KCC-1 structure was not demolished when loaded with Ni metal.

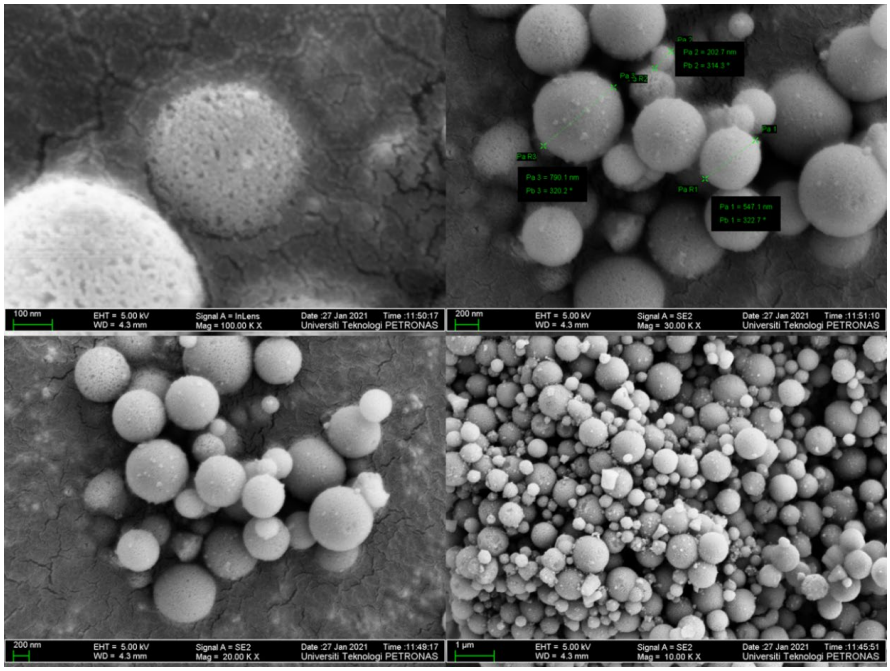

Fig. 2 FESEM image of the catalyst

H_2-TPR Analysis. The metal-support interaction was investigated using the H_2-TPR of the 5Ni/KCC-1. The reduction peak temperatures and the catalysts' reducibility are shown in the Figure 3. The 5Ni/KCC-1 H_2-TPR profile shows a broad reduction peak between temperature 100 – 200 ºC (region IV) in a time frame of 74 – 108 minutes. The lower peak is attributed to the reduction of Ni^{2+} at the catalyst's surface sites or to the reduction of Ni metal that has not been affected by the KCC-1 support while the higher peak refers to a decrease in complex Ni metal species that interact strongly with KCC-1 support. This can be related to the calcination temperature. Three reduction peaks were observed in the TPR profile of the 5Ni/KCC-1 catalyst at 658 ºC, 426 ºC and 406 ºC respectively to the first, second and third peak. The first peak (higher peak) should be linked to the possibility that this is due to the reduction of NiO to Ni, which was affected by the KCC-1 support and the surface lattice of an oxide removal in NiO crystalline. The second peak (region II) is due to the reductions of Ni species with weak 5Ni/KCC-1 interactions as it is unaffected by the KCC-1 support. While the third peak (region III) could be the reductions of Ni species with strong 5Ni/KCC-1 interactions. This indicated that Ni species in low Ni loading catalysts could interact strongly with KCC-1, which was highly stable during the reduction process. Furthermore, the hydrogen consumption of 5Ni/KCC-1 shows multiple reading which are 316.90, 360.54 and 119.39 µmol/g respectively on the first, second and third peak. This means 5Ni/KCC-1 catalyst could be attributed to a reduction in surface NiO with Ni species that have weak and strong interactions with the KCC-1 support. The reason of the high peak, which is strong interaction, is due to high surface area of the catalyst and can have high catalytic performance [19].

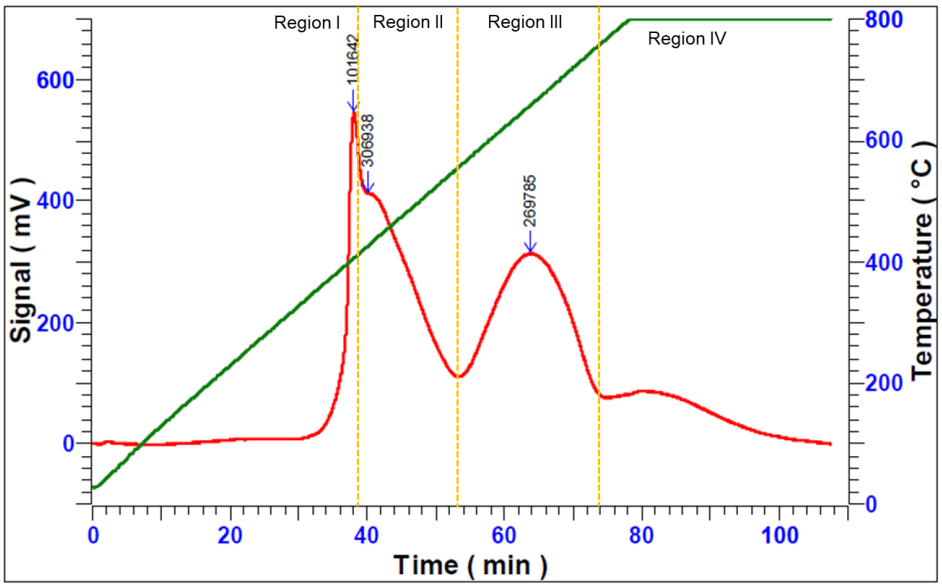

Fig. 3 TPR Profile of 5Ni/KCC-1 Catalyst

Catalyst Performance on DRM. The catalyst was tested for DRM on tubular reactor at different reaction temperatures of 750ºC and 850ºC to evaluate the effect of support morphology and preparation technique on catalyst efficiency in terms of operation and stability. The DRM performance of the 5Ni/KCC-1 catalyst was investigated for 6 h time on stream at 750ºC and 850ºC. Catalysts tested at 850ºC had higher CH_4 and CO_2 conversions than those tested at 750ºC. The 5Ni/KCC-1 catalyst achieved 85.51% and 81.52% of CH_4 and CO_2 conversions within 6 h at 850ºC. A reaction temperature of 750ºC caused CH_4 and CO_2 conversions to fall and decrease to 49.78% and 44.26 % respectively. It shows that carbon formation is more intense at lower temperatures, and at the higher reaction temperature, there is a strong interaction between Ni and KCC-1 that is responsible to prevent sintering and coke deposition [20].

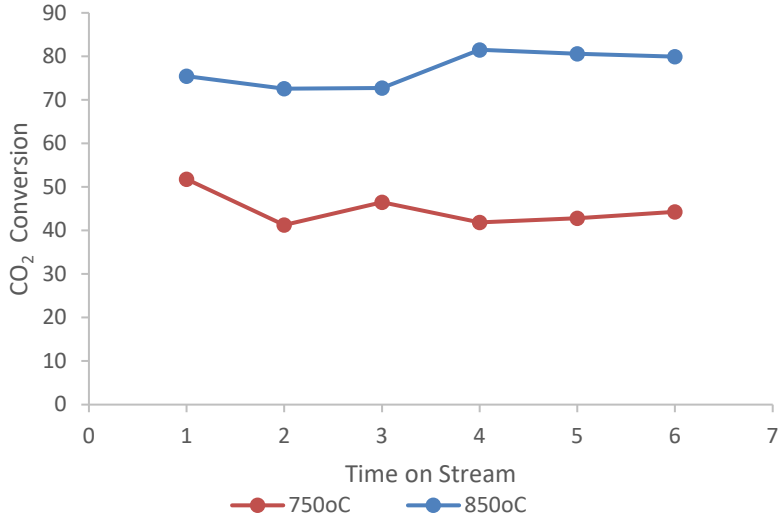

Fig. 4 Conversion of CO_2 at 750ºC and 850ºC

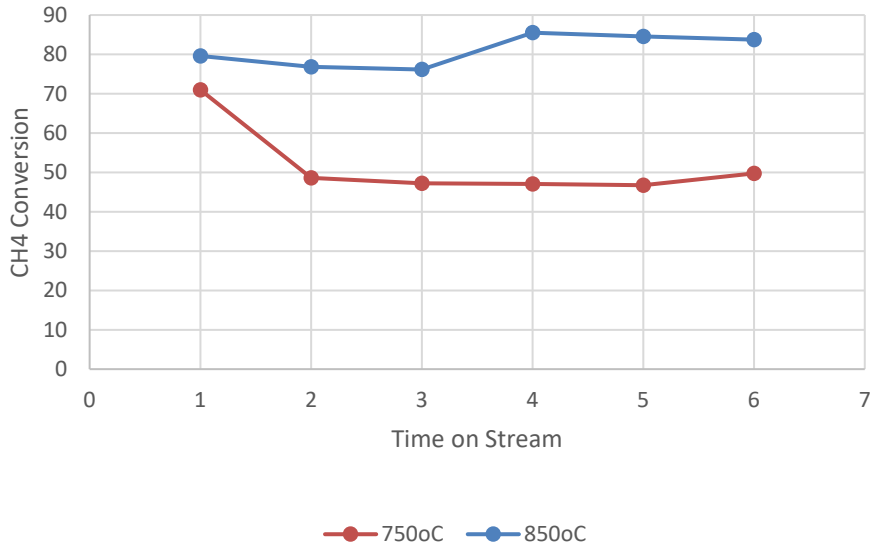

Fig. 5 Conversion of CO_2 at 750°C and 850°C

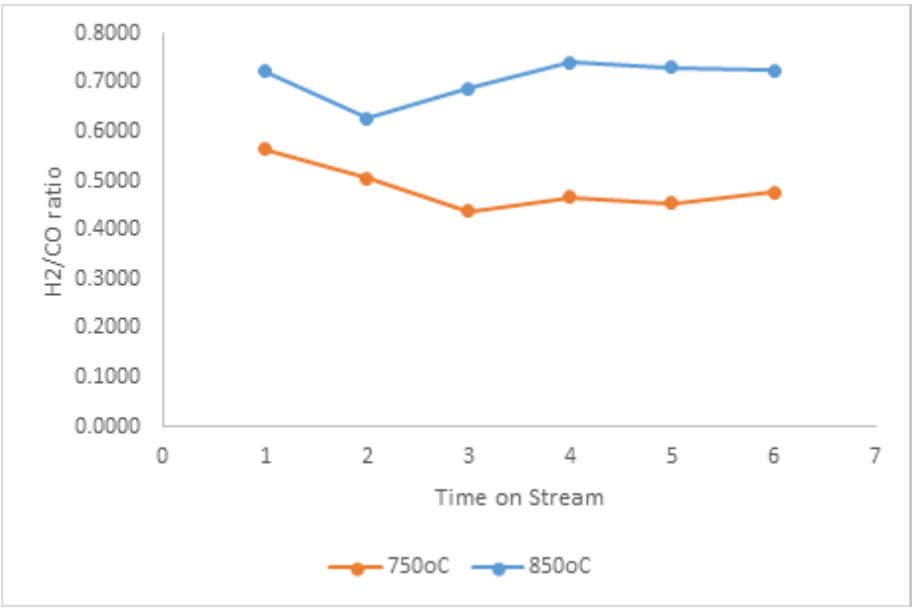

Fig. 6 H_2/CO ratio at different reaction temperature

Conclusions

In the current study, DRM was carried out over 5Ni/KCC-1 catalyst. The catalyst was prepared by ultrasonic assisted impregnation method and was tested for DRM at different temperatures. The catalyst characterization was performed to study the surface area, morphologies, behavior, and active sites of the catalyst. The characterization shows that 5Ni/KCC-1 has a BET surface area and large pore volume which are 456.6031 m^2/g and 0.991964 cm^3/g respectively. FESEM morphology shows that KCC-1 support experienced a well-defined fibrous morphology in a uniform microsphere which can promote high catalytic activity. The catalyst shows higher conversion when operated at 850°C which is 85.51% and 81.52% of CH_4 and CO_2 as compared to the lower reaction temperature. It is proved that conversion increases by increasing the reaction temperature due to less coke formation and high catalyst stability.

Acknowlegement
The authors would like to thank the Collaboration Research Fund (CRF) grant no: 015MD0-010 for providing the financial support and thanks to Universiti Teknologi PETRONAS for providing the research facilities.

References

[1] B. Abdullah, N. A. Abd Ghani, and D. V. N. Vo, "Recent advances in dry reforming of methane over Ni-based catalysts," *J. Clean. Prod.*, vol. 162, pp. 170–185, 2017, https://doi.org/10.1016/j.jclepro.2017.05.176

[2] A. S. Farooqi *et al.*, "Combined H_2O and CO_2 Reforming of CH_4 Over Ca Promoted Ni/Al_2O_3 Catalyst: Enhancement of Ni-CaO Interactions," in *Lecture Notes in Mechanical Engineering*, 2021, pp. 220–229, https://doi.org/10.1007/978-981-16-3641-7_26

[3] B. M. Al–Swai *et al.*, "Low-temperature catalytic conversion of greenhouse gases (CO_2 and CH_4) to syngas over ceria-magnesia mixed oxide supported nickel catalysts," *Int. J. Hydrogen Energy*, vol. 46, no. 48, pp. 24768–24780, 2021, https://doi.org/10.1016/j.ijhydene.2020.04.233

[4] X. Li, "Diversification and localization of energy systems for sustainable development and energy security," *Energy Policy*, vol. 33, no. 17, pp. 2237–2243, 2005, https://doi.org/10.1016/j.enpol.2004.05.002

[5] A. S. Farooqi *et al.*, "Hydrogen-rich syngas production from bi-reforming of greenhouse gases over zirconia modified Ni/MgO catalyst," *Int. J. Energy Res.*, vol. 46, no. 3, pp. 2529–2545, Mar. 2022, https://doi.org/10.1002/er.7325

[6] S. A. Farooqi, A. S. Farooqi, S. Sajjad, C. Yan, and A. B. Victor, "Electrochemical reduction of carbon dioxide into valuable chemicals: a review," *Environ. Chem. Lett.*, 2023, https://doi.org/10.1007/s10311-023-01565-7

[7] J. S. Yu, J. M. Park, J. H. Kwon, and K. S. Park, "Roles of Al_2O_3 coating layer on an ordered mesoporous $Ni/m\text{-}Al_2O_3$ for combined steam and CO_2 reforming with CH_4," *Fuel*, vol. 3, no. July 2022, pp. 37–38, 2023, https://doi.org/10.1016/j.fuel.2022.125702

[8] "Inventory of U.S. Greenhouse Gas Emissions and Sinks | US EPA." .

[9] T. Saelee *et al.*, "Experimental and computational investigation on underlying factors promoting high coke resistance in NiCo bimetallic catalysts during dry reforming of methane," *Sci. Rep.*, vol. 11, no. 1, pp. 1–17, 2021, https://doi.org/10.1038/s41598-020-80287-0

[10] S. Ullah *et al.*, "Sulfur enriched cobalt-based layered double hydroxides for oxygen evolution reactions," *Int. J. Hydrogen Energy*, 2021, https://doi.org/https://doi.org/10.1016/j.ijhydene.2021.09.201

[11] A. Abdulrasheed, A. A. Jalil, Y. Gambo, M. Ibrahim, H. U. Hambali, and M. Y. Shahul Hamid, "A review on catalyst development for dry reforming of methane to syngas: Recent advances," *Renewable and Sustainable Energy Reviews*, vol. 108. pp. 175–193, 2019, https://doi.org/10.1016/j.rser.2019.03.054

[12] A. S. Farooqi *et al.*, "Syngas Production via Bi-Reforming of Methane Over Fibrous KCC-1 Stabilized Ni Catalyst," *Top. Catal.*, vol. 66, no. 1, pp. 235–246, 2023, https://doi.org/10.1007/s11244-022-01713-3

[13] A. S. Farooqi *et al.*, "A comprehensive review on improving the production of rich-hydrogen via combined steam and CO_2 reforming of methane over Ni-based catalysts," *Int. J.*

Hydrogen Energy, vol. 46, no. 60, pp. 31024–31040, 2021, https://doi.org/10.1016/j.ijhydene.2021.01.049

[14] J. Gao, Z. Hou, J. Guo, Y. Zhu, and X. Zheng, "Catalytic conversion of methane and CO_2 to synthesis gas over a La_2O_3-modified SiO_2 supported Ni catalyst in fluidized-bed reactor," *Catal. Today*, vol. 131, no. 1–4, pp. 278–284, 2008, https://doi.org/10.1016/j.cattod.2007.10.019

[15] M. A. Salaev, L. F. Liotta, and O. V. Vodyankina, "Lanthanoid-containing Ni-based catalysts for dry reforming of methane: A review," *Int. J. Hydrogen Energy*, vol. 47, no. 7, pp. 4489–4535, 2022, https://doi.org/10.1016/j.ijhydene.2021.11.086

[16] G. Torres-Sempere *et al.*, "Recent advances on gas-phase CO_2 conversion: Catalysis design and chemical processes to close the carbon cycle," *Curr. Opin. Green Sustain. Chem.*, vol. 36, 2022, https://doi.org/10.1016/j.cogsc.2022.100647

[17] Y. Tian, X. Ma, X. Chen, and C. Zhang, "Effect of Ni-Co bimetallic core-shell catalyst for coke resistance in CO_2 reforming of biomass Tar," *J. Anal. Appl. Pyrolysis*, vol. 164, p. 105539, Jun. 2022, https://doi.org/10.1016/j.jaap.2022.105539

[18] S. N. Bukhari, C. C. Chong, H. D. Setiabudi, Y. W. Cheng, L. P. Teh, and A. A. Jalil, "Ni/Fibrous type SBA-15: Highly active and coke resistant catalyst for CO_2 methanation," *Chem. Eng. Sci.*, vol. 229, p. 116141, 2021, https://doi.org/10.1016/j.ces.2020.116141

[19] A. S. Al-Fatesh *et al.*, "Greenhouse gases utilization via catalytic reforming with Sc promoted Ni/SBA-15," *Fuel*, vol. 330, no. August, p. 125523, 2022, https://doi.org/10.1016/j.fuel.2022.125523

[20] Y. Zhang *et al.*, "Combined steam and CO_2 reforming of methane over Co–Ce/AC-N catalyst: Effect of preparation methods on catalyst activity and stability," *Int. J. Hydrogen Energy*, vol. 47, no. 5, pp. 2914–2925, 2022, https://doi.org/10.1016/j.ijhydene.2021.10.202